Anisotropic sliding of multiple-level biomimetic rice-leaf surfaces on aluminium substrates

Xiaolong Yang[1], Jinlong Song[1], Wenji Xu[1], Xin Liu[1], Yao Lu[2], Yanping Wang[1]

[1]*Key Laboratory for Precision and Non-traditional Machining Technology of the Ministry of Education, Dalian University of Technology, Dalian 116023, People's Republic of China*
[2]*Department of Chemistry, University College London, 20 Gordon Street, London, United Kingdom*
E-mail: wenjixu@dlut.edu.cn

Published in Micro & Nano Letters; Received on 11th September 2013; Revised on 20th October 2013; Accepted on 22nd October 2013

The realisation of special anisotropic sliding behaviour of liquids on metal substrates is very important for applications in fluidic control and water directional transportation. Proposed is a method combining lithography assisted electrochemical etching, anodic oxidation and fluoridation to construct the three-level microstructures (macro/micro/nano) of rice leaves on aluminium. Similar to the natural rice leaf, the prepared surface was endowed with multiple-level microstructures and exhibits superhydrophobicity. The measurements show the biomimetic rice-leaf surface has different anisotropic sliding behaviour with water droplets of different volumes. The perpendicular and parallel sliding angles (SAs) of a 4 µl water droplet were 6.8° and 2.7°, respectively, the anisotropy was 4.1°, which is comparable to that of a natural rice leaf. A mathematical model is presented to explain the mutational significant anisotropy of SAs (10.2°) when the water droplet was only 2 µl. This method is simple and economical, and is believed can be used for the fabrication of large-area biomimetic rice-leaf surfaces on metal.

1. Introduction: Lots of plants and animals in nature exhibit a superhydrophobic property. Their surfaces are capable of making water droplets roll off easily and thereby take away contamination effectively. This particular property is mainly generated by the micro/nanostructures and surface chemistry. For instance, the randomly distributed micropapillaes and waxy branch-like nanostructures endow the lotus with great repellency of water droplets [1]; the elliptic protrusions and nanopins that form the hierarchical structures of the taro leaf have excellent superhydrophobicity [2]; the bristle microstructures allow the water striders to stand on water easily [3]. Inspired by nature, researchers all over the world have devoted significant effort to investigate the mechanism and fabrication of superhydrophobic surfaces. To date, large quantities of superhydrophobic surfaces have been prepared successfully by various methods, including lithography [4, 5], templating [6], laser microfabrication [7], electrochemical machining [8–11], electroless galvanic deposition [12], one-step spray-coating [13] and anodic oxidation [14, 15].

In recent years, the rice leaf has attracted many scientists' attention because of its specific wettability. Its sliding angels (SAs) perpendicular and parallel to the veins are different, at about 3° and 9°, respectively [16]. The anisotropic sliding property makes the natural rice leaf shed water droplets more easily along the longitudinal direction and finally to the root. It is generally believed that the quasi-one-dimensional arrangement of micropapillae covered with nanoscale wax features along the single direction, namely the micro/nanohierarchical structures, results in the observed anisotropic sliding behaviour. Based on this natural phenomenon, many biomimetic anisotropic surfaces that imitate the rice leaf have attracted considerable attention because of their extensive potential applications in microfluidic devices, directional flow control and self-cleaning materials [17–19]. Various methods, including photolithography [20, 21], surface wrinkling [22, 23], electrospinning [24], soft transfer [25] and interference lithography [26, 27], have been applied in fabricating biomimetic rice-leaf surfaces. However, most of the previous research did not realise the dynamic superhydrophobicity, that is, the sliding angle (SA) is too large, even the smallest one along the longitudinal direction can reach 20°.

Lately, Wu *et al.* [16] have proposed a model based on the three-level microstructures (macro/micro/nano) to interpret the anisotropy sliding behaviour through investigating the rice leaf systematically. They realised considerable sliding anisotropy on PDMS (polydimethylsiloxane) by combining photolithography, PDMS imprinting and micro/nano structure coating. The SAs in two directions were 3° and 8°, respectively, successfully mimicking the natural rice leaf. However, this process was complicated, costly and not appropriate for large-scale fabrication. To date, few studies have demonstrated producing the three-level anisotropic surface on metal, which is widely used in industry and agriculture.

In this Letter, a new fabrication method is proposed to prepare the biomimetic rice-leaf surface on Al based on Wu's model. The aluminium (Al) was first electrochemical etched assisted by lithography to gain the oriented sub-millimetre scale groove arrays. The following anodic oxidation generated the micro/nanostructures on the groove arrays. After modification with a low surface energy material, the prepared surface exhibited a great superhydrophobicity with anisotropic sliding behaviour.

It is known that Al and Al alloys are widely used as an important engineering material. Since this method can be used for the fabrication of large-area biomimetic rice-leaf surfaces and the prepared surface has properties of both superhydrophobicity and SA anisotropy, we could possibly apply this technology to water directional transportation. The process could be exploited to obtain multiple-level anisotropic structures economically on Al alloy pipes, and this kind of structures may have potential application in studying the flow field of the pipe. In addition, the surface could also be used as a template to prepare biomimetic rice-leaf surfaces on PDMS.

2. Experiments

2.1. Fabrication of the biomimetic rice-leaf surface: The fabrication process generally consisted of four steps: photolithography, electrochemical etching, anodic oxidation and surface energy reduction (Fig. 1). First, the photopolymer resist film (HT200, 0.04 mm thick, Etemal Chemical Co., China) was stuck onto the polished Al plate (30 × 35 × 2 mm, purity ≥99%, Dalian Al material manufacturer, China) under a certain pressure, and then

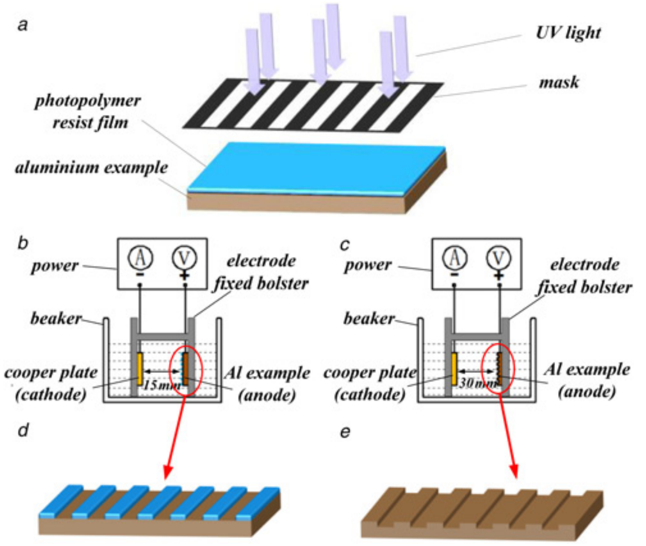

Figure 1 *Schematic illustration of the fabrication process of a biomimetic rice-leaf surface*
a Photolithography process
b Electrochemical etching
c Anodic oxidation
d and *e* Close-up view

exposed for 30 s in a sealed box using a UV lamp (Fig. 1*a*), and developed for 120 s in the eikonogen to obtain the photopolymer sub-millimetre-scale groove arrays on Al; the photopolymer was exploited as a mask in the following etching process. Then, the Al with the mask was used as the anode, whereas a copper (Cu) plate, the same size as the Al specimen, was used as the cathode. Both electrodes were positioned face to face at a distance of 15 mm. The Al was electrochemical etched in a 0.1 M NaCl aqueous solution for 8 min at a current density of 600 mA/cm^2 (Fig. 1*b*) to obtain the Al microgroove arrays. After being electrochemical etched, the Al specimen was ultrasonically rinsed with ethanol to remove the mask. After being anodised in 0.3 M oxalic acid solution for 13 h (Fig. 1*c*), the Al microgroove arrays were covered with the anodic Al oxide (AAO) films, which are composed of superhydrophobic micro/nanostructures. The AAO obtained in our process results in a slight increase in the widths of the grooves and a slight decrease in the heights of the grooves. The grooves retain their morphology after being anodised. The Al specimen was then ultrasonically rinsed with deionised water, subsequently dried and finally immersed in a 1.0 wt% ethanol solution with fluoroalkylsilane for 3 h to lower the surface energy. In this experiment, all the chemicals were of analytical grade.

2.2. Specimen characterisation: The surface morphology of the specimens was characterised by a scanning electron microscope (SEM, JSM-6360LV, Japan). Static contact angles (CAs) and SAs measurements were performed at an ambient temperature using a CA system OCA 20 (Dataphysics Instruments GmbH, Germany) with the sessile-drop method. To characterise the anisotropic dynamic wettability of the biomimetic rice leaf, the CAs perpendicular and parallel to the microgroove arrays were measured with water droplets of different volumes.

3. Result and discussion: First, we investigated the microstructures of the biomimetic rice-leaf surface. Figs. 2*a* and *b* are the top-view SEM images of the biomimetic rice-leaf surface. The sub-millimetre oriented grooves obtained by the process were about 380 µm wide (Fig. 2*a*). The depth of the grooves was about 140 µm (as shown in the inset image of Fig. 2*a*). Fig. 2*c* shows that the surface with microgrooves is covered by uniform hill-like protrusions with sizes of about 20 µm. Many cavities with sizes from 1 to 10 µm are distributed irregularly around these protrusions. A magnified image (Fig. 2*d*) shows that the aforementioned microscale protrusions are composed of flocculent nanoscale structures. After fluoridation, these hierarchical micro/nanostructures have a great static and dynamic superhydrophobicity which mainly results from the discontinuities in the three-phase (solid–liquid–gas) contact line (TCL) because of the trapped air beneath the liquid compared to the smooth structures. It is obvious that this kind of multiple-level biomimetic rice-leaf surface was well prepared, and is similar to the three-level structures of natural rice leaves.

To quantify the static superhydrophobicity, the static CAs were measured. The CAs perpendicular and parallel to the microgrooves were $155° \pm 3°$ (Fig. 2*e*) and $149° \pm 4°$ (Fig. 2*f*), respectively, presenting excellent superhydrophobicity. For the natural rice leaf, the static CAs in two directions were $151° \pm 2°$ and $146° \pm 4°$, respectively [25]. Apparently, the biomimetic rice-leaf surface has a similar superhydrophobicity and anisotropy in CAs, compared with natural rice leaves.

As the unique character of the rice leaf wettability is practically reflected in its anisotropic sliding behaviour, the perpendicular and parallel SAs of water droplets with different volumes were also measured (Fig. 3). When a water droplet stayed on the fabricated biomimetic rice-leaf surface, the surface was tilted until the water droplet started to slide and the inclined angle at this

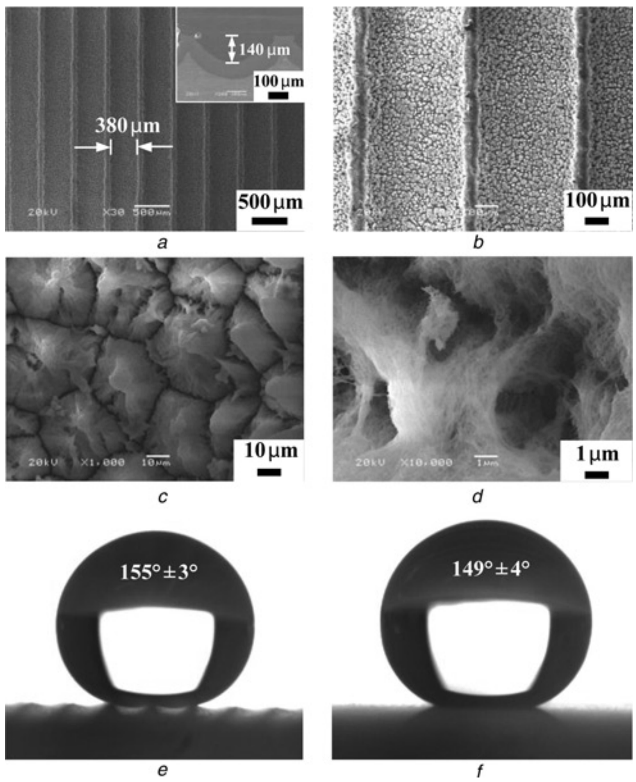

Figure 2 *SEM images of the biomimetic rice-leaf surface and images of static CAs*
a and *b* Top-view SEM images of the biomimetic rice-leaf surface with about 380 µm-wide grooves
The inset image of Fig. 2*a* is the cross-section perpendicular to microgroove arrays
c and *d* Magnified SEM images of the micro/nanostructures on the biomimetic rice-leaf surface
These micro/nanostructures mean that the artificial surface has excellent superhydrophobic properties
e and *f* Static CAs measurements on the biomimetic rice-leaf surface
Figs. 2*e* and *f* illustrate CAs perpendicular and parallel to microgroove arrays, respectively

doi: 10.1049/mnl.2013.0531

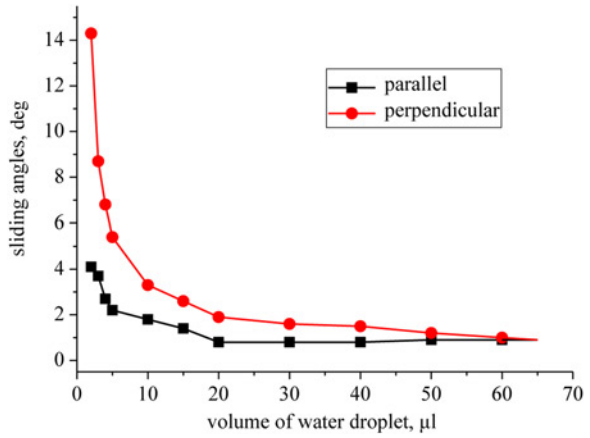

Figure 3 *Perpendicular and parallel SAs of water droplets with different volumes*

moment is defined as the SA. Smaller SA indicates that the surface is slipperier and has a better dynamic wettability. The perpendicular and parallel SAs of the 4 µl water droplet were 6.8° and 2.7°, respectively, the anisotropy was 4.1°, which is comparable to that of a natural rice leaf (6°) [16, 25]. Specially, when the water droplet decreased to 2 µl, the SAs along two directions were 14.3° and 4.1°, respectively, demonstrating significant anisotropy (10.2°). It is apparent that when the droplet volume increased, the SAs parallel and perpendicular to the microgrooves tended to be converged. When the volume of the water droplet was above 60 µl, the sliding anisotropy was not obvious. The SA is closely related to the volume (or mass) of the water droplet and the water repellency of the surface. This relationship is given by Furmidge [28]

$$\sin \alpha = \frac{\omega \gamma_{LV}}{mg} \left(\cos \theta_r - \cos \theta_a\right) \qquad (1)$$

where α is the SA, ω is the width of the droplet, γ_{LV} is the interfacial tension between the liquid and vapour, mg is the gravitational force because of the mass of the droplet and cos θ_r and cos θ_a are the advancing and receding CAs, respectively.

The CA hysteresis perpendicular to the grooves was higher than the values parallel to the grooves because the TCL for water droplet movement perpendicular to the grooves was more discontinuous than that parallel to the grooves because of the higher wetting/dewetting energy barrier [29]. According to (1), this aforementioned anisotropy in CA hysteresis finally resulted in anisotropic SAs of a given volume of water droplet. Based on (1), it could also be inferred that as the droplet volume increased, the effect of the mass became more dominant than the surface tension effect and the CA hysteresis. Therefore, when the water droplet volume increased, the SA decreased, and the SA anisotropy, which was caused by the anisotropic CA hysteresis, would tend to be undifferentiated. This facile transition from anisotropic to isotropic sliding behaviour agreed with the transition of water sliding behaviour observed previously for anisotropic structures [16, 29]. Similarly, as the droplet volume decreased, the surface tension effect and the CA hysteresis became more ascendant than the effect of the mass. Therefore, when the water droplet decreased, the SA increased, and the SA anisotropy would tend to be obvious.

Although the water droplet is small enough (2 µl in this Letter), it could maintain a perfect solid ball shape without any apparent deformation. In this case, the water droplet on the biomimetic rice-leaf surface was set up right between two ridges as shown in Figs. 4*a* and *c*. According to principles of force balance, when the biomimetic rice-leaf surface was tilted along the perpendicular direction, the water droplet would not slide away until its centre

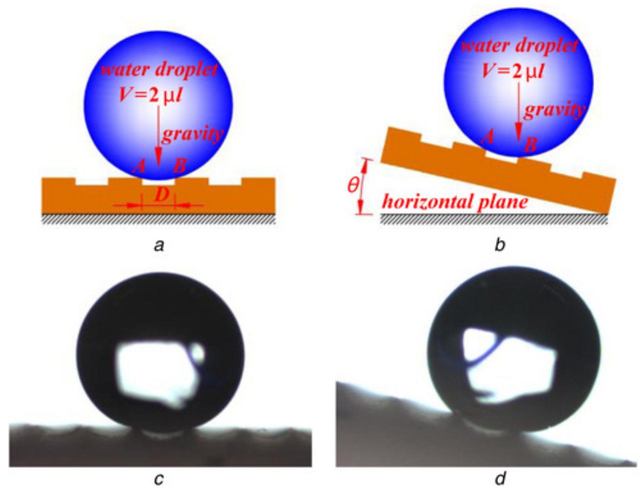

Figure 4 *Illustration of the SA of 2 µl water droplet along the perpendicular direction*
a Water droplet was set up between two ridges, maintaining a perfect solid ball sharp without any apparent deformation
b Water droplet began to slide when the centre of the droplet's gravity crossed the right supporting point 'B'
c and *d* Experimental images

of gravity crossed the left supporting point 'B' in the vertical direction, as illustrated in Figs. 4*b* and *d*. Thus, the SA under this circumstance could be deduced as the following equation

$$\theta = \arcsin \sqrt[3]{\frac{\pi D^3}{6\ V}} \qquad (2)$$

where θ is the SA, D is the width of the grooves ($D = 380$ µm in this Letter), V is the volume of the water droplet. This equation shows that the wider the grooves were or the smaller the volume of the water droplet was, the bigger the perpendicular SA was. Therefore, according to (2), the perpendicular SA of the 2 µl water droplet could be calculated to be 14.1°, which was consistent with the experimental value 14.3°.

Moreover, on the basis of Wu's model, when the widths of the microgrooves are too small (< 100 µm), they could not provide an effective energy barrier to hinder the TCL movement perpendicular to the grooves. Therefore the hysteresis is low so that it could not result in obvious SA anisotropy. As the widths increase to hundreds of micrometres (sub-millimetre scale), the SA anisotropy is distinct because of the high energy barrier. Secondly when the heights of the grooves are too small, the surface also could not exhibit anisotropic sliding behaviour because of the low energy barrier. The SA anisotropy would increase as the heights become larger. However, the anisotropy would not increase when the heights reach a certain critical value, because the water droplet could not reach the bottom of the grooves under this circumstance. In general, the larger the widths and heights of the microgrooves, the more apparent the anisotropic sliding behaviour (here, the SAs were measured with a 4 µl water droplet) [16, 28].

4. Conclusion: A simple method combining lithography assisted electrochemical etching, anodic oxidation and fluoridation is proposed to prepare the three-level (macro/micro/nano) biomimetic rice-leaf surface on Al. The natural rice leaf was mimicked to realise the distinctive anisotropic sliding property. The obtained artificial surface exhibited different anisotropic sliding behaviour with water droplets of different volumes. A mathematical model is presented to explain the mutational significant anisotropy of SAs when the water droplet was as small as 2 µl. These results not only provide an understanding on the anisotropic dynamic behaviour of biomimetic rice-leaf surfaces, but also are serviceable for designing other functional superhydrophobic surfaces for applications in bioinspired systems on metal.

5. Acknowledgment: The authors acknowledge support from the National Natural Science Foundation of China (NSFC, grant 90923022).

6 References

[1] Barthlott W., Neinhuis C.: 'Purity of the sacred lotus, or escape from contamination in biological surfaces', *Planta*, 1997, **202**, pp. 1–8
[2] Guo Z.G., Liu W.M.: 'Biomimic from the superhydrophobic plant leaves in nature: binary structure and unitary structure', *Plant Sci.*, 2007, **172**, pp. 1103–1112
[3] Gao X., Jiang L.: 'Biophysics: water-repellent legs of water striders', *Nature*, 2004, **432**, (7013), p. 36
[4] Chou S.Y., Krauss P.R., Zhang W., ET AL.: 'Sub-10 nm imprint lithography and applications', *J. Vac. Sci. Technol. B, Microelectron. Nanometer Struct.*, 1997, **15**, (6), pp. 2897–2904
[5] Chou S.Y., Keimel C., Gu J.: 'Ultrafast and direct imprint of nanostructures in silicon', *Nature*, 2002, **417**, (6891), pp. 835–837
[6] Yuan Z., Chen H., Tang J., ET AL.: 'A novel preparation of polystyrene film with a superhydrophobic surface using a template method', *J. Phys. D, Appl. Phys.*, 2007, **40**, (11), p. 3485
[7] Wu D., Chen Q.D., Xia H., ET AL.: 'A facile approach for artificial biomimetic surfaces with both superhydrophobicity and iridescence', *Soft Matter*, 2010, **6**, pp. 263–267
[8] Song J.L., Xu W.J., Lu Y., ET AL.: 'Rapid fabrication of superhydrophobic surfaces on copper substrates by electrochemical machining', *Appl. Surf. Sci.*, 2011, **257**, (24), pp. 10910–10916
[9] Song J.L., Xu W.J., Lu Y.: 'One-step electrochemical machining of superhydrophobic surfaces on Al substrates', *J. Mater. Sci.*, 2012, **47**, (1), pp. 162–168
[10] Lu Y., Song J.L., Liu X., ET AL.: 'Preparation of superoleophobic and superhydrophobic titanium surfaces via an environmentally friendly electrochemical etching method', *ACS Sustain. Chem. Eng.*, 2012, **1**, (1), pp. 102–109
[11] Lu Y., Song J.L., Liu X., ET AL.: 'Loading capacity of a self-assembled superhydrophobic boat array fabricated via electrochemical method', *Micro Nano Lett.*, 2012, **7**, (8), pp. 786–789
[12] Xu X., Zhang Z., Yang J.: 'Fabrication of biomimetic superhydrophobic surface on engineering materials by a simple electroless galvanic deposition method', *Langmuir*, 2009, **26**, (5), pp. 3654–3658
[13] Momen G., Farzaneh M.: 'Simple process to fabricate a superhydrophobic coating', *Micro Nano Lett.*, 2011, **6**, (6), pp. 405–407
[14] Shibuichi S., Yamamoto T., Onda T., ET AL.: 'Super water-and oil-repellent surfaces resulting from fractal structure', *J. Colloid Interface sci.*, 1998, **208**, (1), pp. 287–294
[15] Mateo J.N., Kulkarni S.S., Das L., ET AL.: 'Wetting behavior of polymer coated nanoporous anodic alumina films: transition from super-hydrophilicity to super-hydrophobicity', *Nanotechnology*, 2011, **22**, (3), p. 035703
[16] Wu D., Wang J.N., Wu S.Z., ET AL.: 'Three-level biomimetic rice-leaf surfaces with controllable anisotropic sliding', *Adv. Funct. Mater.*, 2011, **21**, (15), pp. 2927–2932
[17] Gau H., Herminghaus S., Lenz P., ET AL.: 'Liquid morphologies on structured surfaces: from microchannels to microchips', *Science*, 1999, **283**, (5398), pp. 46–49
[18] Zhao B., Moore J.S., Beebe D.J.: 'Surface-directed liquid flow inside microchannels', *Science*, 2001, **291**, (5506), pp. 1023–1026
[19] Higgins A.M., Jones R.A.L.: 'Anisotropic spinodal dewetting as a route to self-assembly of patterned surfaces', *Nature*, 2000, **404**, (6777), pp. 476–478
[20] Morita M., Koga T., Otsuka H., ET AL.: 'Macroscopic-wetting anisotropy on the line-patterned surface of fluoroalkylsilane monolayers', *Langmuir*, 2005, **21**, (3), pp. 911–918
[21] Sommers A.D., Jacobi A.M.: 'Creating micro-scale surface topology to achieve anisotropic wettability on an Al surface', *J. Micromechan. Microeng.*, 2006, **16**, (8), p. 1571
[22] Chung J.Y., Youngblood J.P., Stafford C.M.: 'Anisotropic wetting on tunable micro-wrinkled surfaces', *Soft Matter.*, 2007, **3**, (9), pp. 1163–1169
[23] Lee S.G., Lim H.S., Lee D.Y., ET AL.: 'Tunable anisotropic wettability of rice leaf-like wavy surfaces', *Adv. Funct. Mater.*, 2012, pp. 547–553
[24] Wu H., Zhang R., Sun Y., ET AL.: 'Biomimetic nanofiber patterns with controlled wettability', *Soft Matter*, 2008, **4**, (12), pp. 2429–2433
[25] Yao J., Wang J.N., Yu Y.H., ET AL.: 'Biomimetic fabrication and characterization of an artificial rice leaf surface with anisotropic wetting', *Chin. Sci. Bull.*, 2012, **57**, (20), pp. 2631–2634
[26] Zhao Y., Lu Q., Li M., ET AL.: 'Anisotropic wetting characteristics on submicrometer-scale periodic grooved surface', *Langmuir*, 2007, **23**, (11), pp. 6212–6217
[27] Xia D., Brueck S.R.J.: 'Strongly anisotropic wetting on one-dimensional nanopatterned surfaces', *Nano Lett.*, 2008, **8**, (9), pp. 2819–2824
[28] Furmidge C.G.L.: 'Studies at phase interfaces. I. The sliding of liquid drops on solid surfaces and a theory for spray retention', *J. Colloid Sci.*, 1962, **17**, (4), pp. 309–324
[29] Yoshimitsu Z., Nakajima A., Watanabe T., ET AL.: 'Effects of surface structure on the hydrophobicity and sliding behavior of water droplets', *Langmuir*, 2002, **18**, (15), pp. 5818–5822

doi: 10.1049/mnl.2013.0531